

Experimental and theoretical evaluation of the phonon thermal conductivity of niobium at intermediate temperatures

R. K. Williams, W. H. Butler, R. S. Graves, and J. P. Moore

Metals and Ceramics Division, Oak Ridge National Laboratory, Oak Ridge, Tennessee 37830

(Received 2 December 1982; revised manuscript received 24 August 1983)

The thermal conductivity, electrical conductivity, and thermopower of Nb and four Nb-based alloys were measured over the temperature range 80–400 K. The thermal- and electrical-conductivity data were used to define the roles of phonon-phonon and phonon-electron scattering in limiting the phonon thermal conductivity. The phonon-electron thermal resistance was compared with the results of a new first-principles calculation. As expected from the high superconducting transition temperature, phonon-electron scattering is quite strong in Nb. The theoretical calculation reproduces the results of an earlier low-temperature experiment, but gives only about $\frac{2}{3}$ of the scattering strength derived from the intermediate-temperature data. This discrepancy is just inside the experimental error limits, but some possible explanations of the difference are discussed.

I. INTRODUCTION

Phonons can make a significant contribution to the measured thermal conductivity of a metallic conductor, and an understanding of this contribution is important for making estimates of the thermal transport properties of new materials and for improving our understanding of the electron-phonon interaction in the metallic elements. The results described in this paper are part of a systematic effort to develop methods for identifying the phonon contribution λ_{ph} and to strengthen the connection between the measurements and theory. Niobium is particularly useful as a test of our understanding of λ_{ph} because it has been extensively studied, both theoretically and experimentally. Niobium is also interesting because of its high superconducting transition temperature, which is indicative of strong electron-phonon scattering. This scattering should also be important in limiting λ_{ph} .

The experimental techniques and methods used to analyze the data have been described before.^{1,2} This paper contains sections describing the Nb and Nb-alloy samples, the experimental results, and a discussion of the results. Measurements at high temperature for Nb have been reported previously.³ Most of the final section is devoted to λ_{ph} and contains a first-principles evaluation of the resistance to phonon transport due to interactions with the electron gas. This treatment follows earlier calculations⁴ of the electronic thermal conductivity λ_e and electrical resistivity ρ of Nb. The comparison between theory and experiment is the central point of this paper.

II. SAMPLE PREPARATION AND CHARACTERISTICS

The 6-mm-diam Nb sample was machined from a rod of low-Ta material that had been electron-beam zone refined by Reed.⁵ After machining to produce a uniform (± 0.0025 mm) diameter, the sample was annealed for 48 h

at 2273 K in an ultrahigh-vacuum furnace. The ice-point electrical resistivity of this sample was 0.67% lower than the value obtained by White and Woods,⁶ and the thermal conductivity was within about 2% of that measured by Merisov *et al.*⁷ over the temperature range 100–273 K. Our thermal conductivity values are about 6–10% lower over this same range than those recommended by Ho *et al.*⁸ in their compilation. The reason for this discrepancy seems to be that the recommended $\lambda(T)$ values were obtained by fitting lower-temperature data to an approximate formula and extrapolating.

The alloy samples were prepared from electron-beam melted Nb and Mo and crystal bar Zr. Charges were repeatedly arc melted in a gettered argon atmosphere to promote homogeneity and then dropcast into rods about 20 mm in diameter. The (7–8)-mm-diam samples were cut from the outer portions of the castings in order to avoid center line porosity. All of the samples were given a 24-h, 1973-K homogenization anneal in an ultrahigh-vacuum furnace. Metallographic examination showed large (1–5 mm) grains with no evidence of coring.

Measurements of the physical characteristics of the samples are summarized in Table I. The concentrations of Mo and Zr were determined by a colorimetric method. A complete impurity analysis of the 4.5 at.% Mo–5.1 at.% Zr sample showed that the major impurities (wt. ppm) were as follows: C, 47; H, 4; N, 48; O, 29; Cu, 4; Fe, 2; Hf, 10; Pt, 20; S, 0.2; V, 3; Ta, 2000; and W, 500.

III. EXPERIMENTAL VALUES

Smoothed thermal conductivity (λ) and electrical resistivity (ρ) values for the five samples are shown in Table II. Seebeck coefficient data are plotted in Fig. 1. The higher (300–400 K) temperature ρ data for some of the samples differ from our earlier³ values by small ($\leq 0.8\%$) amounts. These differences were caused by favoring the

TABLE I. Sample characteristics.

	Zone-refined Nb	Nb— 5.1 at. % Mo	Nb— 10.0 at. % Mo	Nb—2.4 at. % Mo— 2.4 at. % Zr	Nb—4.8 at. % Mo— 5.1 at. % Zr
Vacuum annealing time (h)	48	24	24	24	24
Temperature (K)	2273	1973	1973	1973	1973
Density (10^{-3} kg/m ³)		8.662	8.741	8.548	8.547
Lattice parameter (10^{-10} m)		3.293	3.282	3.304	3.315
Superconducting transition temperature (K)		7.72	6.26	8.32	8.23
Residual resistivity (10^{-8} Ω m)	0.0457	2.87	5.09	5.45	7.18
Sample uniformity, range of three resistivity measurements at different positions (%)	0.04	0.03	0.02	0.21	0.22

knife-edge⁹ ρ data and using additional data from the low-temperature absolute longitudinal heat-flow^{10,11} apparatus. The estimated uncertainties and experimental techniques have been discussed previously.^{10,11} The property values shown in Table II contain extra digits to eliminate rounding errors. The λ values for Nb—5 at. % Mo, Nb—10 at. % Mo, and Nb—2.4 at. % Mo—2.4 at. % Zr were also checked by making measurements on smaller companion samples with a comparative method⁹ over the temperature range 305–360 K.

IV. DISCUSSION

The principal goal of this study was to determine the phonon thermal conductivity λ_{ph} of Nb at intermediate temperatures. This result is part of a systematic study^{1,2} of the phonon and electronic thermal conductivities of the bcc transition elements and takes on an added significance because recent theoretical advances⁴ have led to truly first-principles calculations of the phonon resistance due to electron-phonon scattering W_{e-ph} . It appears that λ_{ph} measurements give a relatively good test of this theory. This section begins with a consideration of the electrical resistivity, the principal goal being to generate experimental parameters that are employed in deriving λ_{ph} estimates. The sections on phonon conductivity follow a brief consideration of the Seebeck coefficient data. The electronic thermal conductivity values, which have been discussed elsewhere,⁴ are also included.

A. Electrical resistivity

The experimentally observed composition and temperature dependence of the electrical resistivity ρ is given in Table II. We found it convenient to parametrize the temperature dependence of each alloy by use of the formula

$$\rho = A + \rho_{BG} \left[R, \frac{T}{\Theta_R} \right] - BT^2, \quad (1)$$

where A and B are fitting parameters and ρ_{BG} is the Bloch-Grüneisen formula for the ideal electrical resistivity,

$$\rho_{BG} = 4R \left[\frac{T}{\Theta_R} \right]^5 J_5 \left[\frac{\Theta_R}{T} \right], \quad (2)$$

$$J_n(x) = 2^{n-1} \int_0^{x/2} dy y^{n-2} \frac{y^2}{\sinh^2 y}. \quad (3)$$

Table III displays the parameters A , B , Θ_R , and R/Θ_R obtained by means of a least-squares fit of the data in Table II to Eq. (1). The reader should be cautioned that Eq. (1) should not be expected to be valid outside the

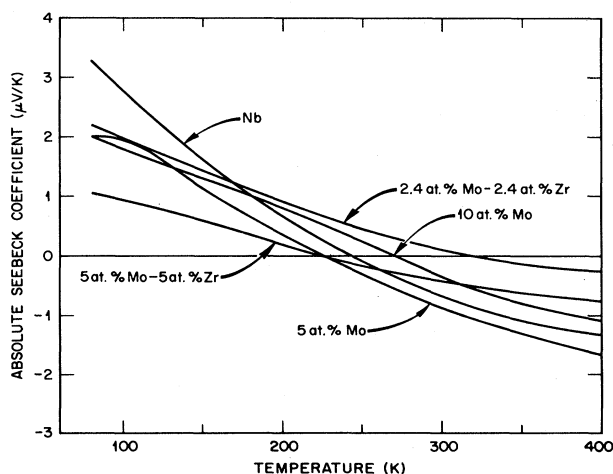


FIG. 1. Absolute Seebeck coefficient values for zone-refined Nb and four Nb-based alloys.

TABLE II. Smoothed thermal conductivity and electrical resistivity values: λ (W/m K), and ρ (10^{-8} Ω m).

Temperature (K)	Zone-refined Nb		Nb-5 at. % Mo		Nb-10 at. % Mo		Nb-2.4 at. % Mo-2.4 at. % Zr		Nb-5 at. % Mo-5 at. % Zr	
	λ	ρ	λ	ρ	λ	ρ	λ	ρ	λ	ρ
80	52.34	2.7235	33.25	5.309	26.33	7.349	23.41	8.170	19.57	10.091
100	49.83	3.966	35.42	6.436	29.26	8.395	25.98	9.375	22.04	11.318
120	49.35	5.189	37.33	7.544	31.72	9.427	28.12	10.541	24.16	12.488
140	49.49	6.371	39.04	8.625	33.85	10.422	30.00	11.677	26.05	13.615
160	49.78	7.517	40.55	9.669	35.74	11.390	31.64	12.765	27.77	14.703
180	50.14	8.625	41.88	10.684	37.42	12.334	33.11	13.823	29.32	15.746
200	50.49	9.703	43.02	11.671	38.90	13.253	34.41	14.855	30.71	16.757
220	50.89	10.752	44.02	12.634	40.22	14.205	35.57	15.858	31.98	17.737
240	51.24	11.771	44.94	13.576	41.42	15.152	36.63	16.831	33.15	18.687
260	51.53	12.769	45.79	14.499	42.53	16.016	37.61	17.783	34.24	19.614
280	51.84	13.746	46.59	15.404	43.57	16.817	38.52	18.717	35.26	20.521
300	52.12	14.705	47.33	16.291	44.55	17.535	39.37	19.636	36.22	21.413
320	52.46	15.647	48.02	17.166		18.346	40.17	20.547	37.14	22.290
340	52.77	16.572	48.66	18.029		19.138	40.92	21.439	37.99	23.147
360	53.08	17.482	49.26	18.878		19.925	41.61	22.311	38.80	23.987
380	53.34	18.376	49.82	19.716		20.706	42.26	23.166	39.56	24.818
400	53.52	19.258	50.33	20.536		21.482	42.84	24.016	40.27	25.634

TABLE III. Parameters derived from least-squares fits of the smoothed resistivity data (Table II) to the equation $\rho = A + \rho_{BG} - BT^2$ ($\Theta_R = \text{const}$).

Material	Average percent deviation of calculated values		A^a (10^{-8} Ω m)	Residual resistivity (10^{-8} Ω m)	B (10^{-13} Ω m/K ²)	R/Θ_R (10^{-8} Ω m/K)	Θ_R (K)	Θ_D^b (K)
Zone-refined Nb	0.05		0.0457 ^c	0.0457	1.765	0.05622	245	280
Nb-5.1 at. % Mo	0.02		3.0	2.87	1.346	0.05034	256	288
Nb-10.0 at. % Mo	0.23		5.51	5.09	1.355	0.04682	293	296
Nb-2.4 at. % Mo-2.4 at. % Zr	0.03		5.45	5.45	1.683	0.05409	229	277
Nb-4.8 at. % Mo-5.1 at. % Zr	0.06		7.3	7.18	2.051	0.05490	222	273

^aExperimental residual resistivity values are shown in Table I.^bThese literature values are discussed in the text.^cFor Nb the constant term forced to equal ρ_0 .

range 80–400 K. We do find empirically that A is in reasonable agreement with the independently measured residual resistivity, which is also given in Table III. The small (positive) differences are probably due to deviations from Matthiessen's rule, but they may also be partly attributable to limitations of the Bloch-Grüneisen fitting formula. Note also that the ρ_0 values (Table I) show that Zr additions produce larger effects than Mo. The effect also seems to be about 50% larger than the observations for the analogous Hf-Ta-W series,² even though the size differences are very similar in both series. Additional studies of binary Ta-Hf and Nb-Zr alloys are required to clarify this point.

The term $-BT^2$ in Eq. (1) is especially interesting. In our parametrization of the experimental data this term merely expresses the fact that the resistivity does not increase as fast at high temperature as one would expect from the Bloch-Grüneisen formula. This phenomenon has been called a deviation from linearity (DFL).^{12,13} Actually ρ/T , which should be a monotonically increasing function of T according to Boltzmann theory, has a maximum near 300 K for Nb. Several explanations for this "saturation" effect have been offered, among them are "phonon softening," "Mott-Fermi smearing," and "interband transitions."¹² It has not yet been established which, if any, of these explanations is responsible for the effect. The DFL complicates comparisons between theoretical calculations⁴ and experiment because it is not included in the first-principles theory.

The characteristic temperatures Θ_R derived from the data show compositional trends similar to the Θ_D values obtained from the literature, but Θ_R varies more rapidly with composition than Θ_D . The Θ_D values for Nb-Mo alloys shown in Table III are from Powell *et al.*¹⁴ and are appropriate for intermediate temperatures. The data of Ishikawa and Cappelletti¹⁵ show that the low-temperature Θ_D values for the isoelectronic alloys containing Mo and Zr are only slightly less than those of pure Nb. We estimated the intermediate-temperature Θ_D values for these alloys by multiplying the low-temperature Θ_D values of Ref. 15 by the ratio of the intermediate- and low-temperature Θ_D value of Nb.

At high temperatures, the Bloch-Grüneisen formula for ρ approaches $(R/\Theta_R)T$, and the R/Θ_R values show com-

position changes similar to those observed for Ta alloys.² The decrease produced by Mo additions can be predicted from the changes in the superconducting transition temperature T_c .^{3,16} The isoelectronic alloys show much smaller R/Θ_R decreases ($\sim 4\%$), and this is also about what would be predicted from the shifts in the mass enhancement factor Λ .¹⁵ Butler¹⁷ has discussed the three factors responsible for these changes in Λ and R/Θ_R . The R/Θ_R value shown in Table III yields a Λ_{tr} value for Nb of 1.10. Typical literature values for this parameter are 0.96–1.04.¹⁸

B. Thermopower

Smoothed values for the thermopower of Nb and for the four alloys are given in Fig. 1 for temperatures between 80 and 400 K. Presumably the observed thermopower consists of a positive phonon drag term, which predominates around 80 K, plus a negative diffusion term which varies approximately linearly in T . The phonon drag term contains valuable information about the ratio of the phonon-electron scattering rate to the total phonon scattering rate.¹⁹ Unfortunately, we are unable to separate the two contributions. Low-temperature thermopower measurements would be very helpful in this regard, as would a serious first-principles calculation of either component. We report the data in this paper for completeness, and because this property is useful in checking the consistency of thermal conductivity measurements.

C. Phonon thermal conductivity (experimental)

The electrical and thermal conductivity data (Table II) for Nb and the four Nb-based alloys were used to estimate the phonon conductivity for Nb. The technique which we used was the same as was used recently to determine the phonon thermal conductivity of Ta.² It requires solving the following two equations for L (the electronic Lorenz function for electron-phonon scattering) and λ_{ph}^{Nb} the phonon thermal conductivity of Nb:

$$\lambda^{Nb} = \left[\frac{\rho_0}{L_0 T} + \frac{\rho(Nb) - \rho_0}{LT} \right]^{-1} + \lambda_{ph}^{Nb}, \quad (4)$$

TABLE IV. Parameters used in evaluating the ratio of the phonon conductivities of niobium and its alloys.

Material	Θ_D (K)	$\lim_{T \rightarrow \infty} W_{e-ph}^a$ (deg m/W)	Grüneisen constant	Mean atomic mass (kg)	Mean atomic size (m)	Scattering parameter Γ^b
				($\times 10^{25}$)	($\times 10^{10}$)	
Nb	280	0.201	1.74	1.543	2.620	
Nb–5 at. % Mo	288	0.178	1.736	1.545	2.614	4.27×10^{-3}
Nb–10 at. % Mo	296	0.158	1.731	1.548	2.605	8.04×10^{-3}
Nb–2.4 at. % Mo–2.4 at. % Zr	277	0.196	1.715	1.543	2.622	1.04×10^{-2}
Nb–5 at. % Mo–5 at. % Zr	273	0.191	1.715	1.544	2.631	1.60×10^{-2}

^a W_{∞} in Eq. (9).

^bPhonon-solute scattering parameter as defined by Abeles (Ref. 25).

$$\lambda^A = \left[\frac{A}{L_0 T} + \frac{\rho(A) - A}{LT} \right]^{-1} + \beta \lambda_{ph}^{Nb}. \quad (5)$$

In these equations L_0 is the Lorenz number for elastic scattering²⁰ ($L_0 = 2.443 \times 10^{-8} \text{ V}^2/\text{K}^2$), λ^{Nb} and λ^A are the measured thermal conductivities of Nb and one of the alloys, and $\rho(Nb)$ and $\rho(A)$ are the corresponding electrical resistivities. The quantities ρ_0 and A are the residual resistivities of Nb and the alloy, respectively. The quantity β is defined to be the ratio of the phonon thermal conductivity of the alloy to the phonon thermal conductivity of Nb and is calculated as described below. The remaining quantities L , the ideal Lorenz function, and λ_{ph}^{Nb} the phonon thermal conductivity are determined by solving the two equations.

Equations (4) and (5) state that the thermal conductivity is the sum of an electronic part and a phonon part. The electronic thermal resistance is assumed to be the sum of an impurity part ($\rho_0/L_0 T$ for Nb) and an electron-phonon part. The equations also assume that L , the Lorenz function for electron-phonon scattering, is the same in the alloys as in pure Nb.

In the alloy method for determining phonon thermal conductivities of metals it is usually assumed that λ_{ph} is the same in the dilute alloy as in the pure metal. This amounts to setting β equal to unity in Eq. (5). Here, as in Ref. 2, we have tried to improve upon this assumption by estimating the changes in electron-phonon, phonon-phonon, and point-defect scattering which occur on alloying. The ratio of the alloy phonon thermal conductivity to that of Nb is given by

$$\beta = \frac{W_{e-ph}(Nb) + W_{ph-ph}(Nb)}{W_{e-ph}(\text{alloy}) + W_c}, \quad (6)$$

where W_{e-ph} and W_{ph-ph} are phonon thermal resistivities due to electron-phonon and phonon-phonon scattering, respectively. W_c is the combined thermal resistance in the alloy due to phonon-phonon and phonon-impurity scattering. The phonon resistance due to electron-phonon scattering was calculated from^{21,22}

$$W_{e-ph} = \frac{W_\infty}{2} \left[\frac{\Theta_D}{T} \right]^2 J_3^{-1} \left[\frac{\Theta_D}{T} \right], \quad (7)$$

where W_∞ is the high-temperature limit of W_{e-ph} . The W_∞ values used for niobium and the alloys are shown in Table IV. The method used to obtain these estimates has been described previously.² The phonon-phonon scattering in Nb, $W_{ph-ph}(Nb)$, was calculated from the Leibfried-Schlömann formula:^{23,24}

$$W_{ph-ph}(Nb) = 5.88 \times 10^{-27} \frac{\gamma^2}{M \delta \Theta_D^3} T, \quad (8)$$

in units of deg m W^{-1} . In this formula γ is the Grüneisen constant, δ is the cube root of the volume per atom, and M is the atomic mass. The combined scattering in the alloys, W_c , was calculated from Abeles's²⁵ formula using the impurity scattering cross sections shown in Table IV. This calculation assumes that the ratio of N - to U -process relaxation times is 9:5, and that the lattice strain scatter-

ing parameter is 40.²⁵

The values of β determined in this way are decreasing functions of temperature. They increase with the addition of Mo and decrease with the addition of Zr. They range from 1.10 for the 10 at. % Mo alloy at 80 K to 0.74 for the 5 at. % Mo–5 at. % Zr alloy at 400 K.

Figure 2 shows λ_{ph} for Nb as determined from the experimental data using Eqs. (4) and (5). Figure 2(a) shows the λ_{ph} values determined using $\beta=1$ in Eq. (5), and Fig. 2(b) shows λ_{ph} for Nb when account is taken of the change in λ_{ph} on alloying through the parameter β . Inclusion of β in Eq. (5) reduces the scatter between λ_{ph}^{Nb} derived using different alloys by a factor of 2.5. It also seems to give a result which is more realistic at higher temperatures. The solid line in Fig. 2(b) represents our best experimental estimate of the phonon conductivity of Nb.

The uncertainty associated with the λ_{ph}^{Nb} curve has two components. The experimental part, which has been extensively discussed,² arises because the λ and ρ values have associated uncertainties, and the λ_{ph} values are obtained by solving two equations containing λ , ρ , and T measurements on two samples. Both maximum determinate errors and statistical analyses indicate that this uncertainty is about $\pm 40\%$ at 100 K.² The second component, failure of the model [Eqs. (4) and (5)] due to, for example, a change in L on alloying, seems to be a less important source of error. From an analysis of Eqs. (4) and (5) one can estimate the effect on λ_{ph}^{Nb} of a small change in L due to alloying. For the 5 at. % Mo alloy we find, for example, that a 1% change in L causes a change in λ_{ph}^{Nb} of 0.7%, 1.8%, and 2.9% at 100, 200, and 300 K, respectively.

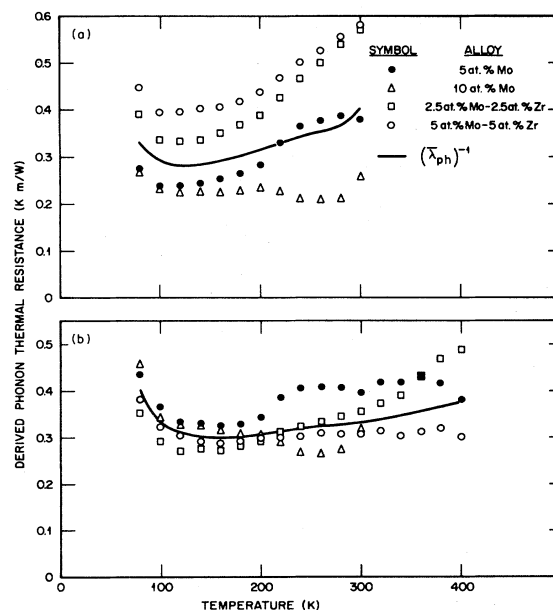


FIG. 2. Temperature dependence of the phonon thermal resistance (λ_{ph}^{-1}) of niobium. The methods used to obtain parts (a) and (b) are described in the text.

The phonon thermal resistance shown in Fig. 2 is the sum of the resistance due to phonon-phonon scattering (which should increase linearly with temperature in this temperature range),²⁴ and the resistance due to phonon-electron scattering (which should be approximately constant).²⁰ It is clear from Fig. 2 that the latter resistance is dominant. This is not surprising since the electron-phonon interaction is known to be particularly strong in Nb.

Assuming that the phonon-phonon resistance increases linearly with T , which is justified above about 70 K,²⁴ and that the temperature dependence of the electron-phonon resistance, W_{e-ph} , can be obtained from a simple Debye-type formula^{21,22} [Eq. (7)]:

$$\lambda_{ph}^{-1}(Nb) = \alpha T + \frac{W_{\infty}}{2} \left[\frac{280}{T} \right]^2 / J_3 \left[\frac{280}{T} \right]. \quad (9)$$

Fitting the λ_{ph} values from Fig. 2(b) to this formula yields

$$\alpha = 2.87 \times 10^{-4},$$

in units of m/W , and

$$W_{\infty} = 0.234,$$

in units of $\text{deg } m/W$. The fit is excellent, with an average difference of only 3%. This treatment indicates that the phonon conductivity maximizes at about 150 K. For Ta,² the maximum is located at a lower temperature, and the difference is readily understood in terms of Eq. (9).

The phonon-phonon scattering term α is about 40% larger than the value calculated by using the parameters shown in Table IV and the modified²³ Leibfried-Schlömann equation. This is satisfactory because the parameter is not well defined by the experimental result, and the equation tends to underestimate the experimental thermal resistance.²⁶ The electron-phonon resistance is about four times larger than the value derived from the experimental data of Sousa.^{22,27}

D. Phonon thermal conductivity (theoretical)

Recently it has become possible to calculate the component of the phonon linewidth in a metal which arises from electron-phonon scattering.^{28,29} Since the lifetime of a phonon of momentum q and mode index j , $\tau_j(q)$, is inversely proportional to its linewidth, $\gamma_j(q)$, i.e.,

$$\tau_j(q) = \hbar / \gamma_j(q), \quad (10)$$

one needs only to know the phonon linewidth and the phonon dispersion to calculate the lattice thermal conductivity,^{21,22}

$$(W_{e-ph})^{-1} = \frac{1}{2\Omega_a} \sum_{j,q} C_j(q, T) u_{jx}^2(q) \hbar / \gamma_j(q), \quad (11)$$

$$C_j(q, T) = \frac{k_B X^2 e^X}{(e^X - 1)^2} \quad X = \hbar \omega_j(q) / k_B T, \quad (12)$$

$$u_{jx}(q) = \frac{\partial \omega_j(q)}{\partial q_x}. \quad (13)$$

This formula implies that comparison of measured and calculated W_{e-ph} values offers a relatively direct test of the theoretical model. The equation only requires information about the phonon dispersion curves which can be obtained from experiment and the phonon lifetime which is evaluated from theory.

We used the linewidths calculated in Ref. 28 to calculate the thermal conductivity of Nb using Eq. (11). The phonon frequencies and velocities were determined by a Born-von Kármán model fit to the experimentally determined dispersion curves.¹⁴ The linewidths taken from the work of Ref. 28 and used in Eq. (11) contain a significant approximation in that the rigid muffin-tin approximation was used to calculate the electron-phonon matrix elements. We know something about the accuracy of these linewidths, however, since they have been compared directly with experiment³⁰ and have been used to calculate the superconducting and transport properties of Nb.^{4,18}

Given the linewidth, the evaluation of Eq. (11) is quite straightforward. We used 728 points in the irreducible $\frac{1}{48}$ th wedge of the Brillouin zone on a cubic mesh in order to perform the sum. The result is shown in Fig. 3. Also included is the "constant- α^2 " approximation which was used previously²² to treat the interelement variation of W_{e-ph} . The calculations merge at high temperatures, but the constant- α^2 formula gives W_{e-ph} values about a factor of 2 too high at low temperatures. The new W_{e-ph} calculations are supported by the low-temperature data of Sousa.²⁷ This suggests that the consistent differences²² between low- and intermediate-temperature W_{e-ph} values may be attributed to failure of the interpolation formula based on the constant- α^2 approximation.

E. Electronic thermal conductivity

The electronic thermal conductivity of Nb can be obtained by subtracting the λ_p values estimated in Secs. IV C and IV D from the experimental thermal conductivity data. Figure 4 (curve labeled experiment) shows the intrinsic electronic thermal resistance, W_{ei} , obtained in this manner after applying a small correction for impurity scattering ($W_{ei} = W_e - \rho_0 / L_0 T$). The resultant curve has a maximum at 130 K and decreases linearly at higher temperature. The negative high-temperature slope and the position of the maximum in W_{ei} are quite insensitive to errors in estimating λ_{ph} .

This experimentally determined curve should be compared with the other curve in Fig. 4 (labeled theory), which shows the calculated results of Pinski *et al.*⁴ This calculation (and any calculation based on ordinary Boltzmann theory) yields a W_{ei} curve that is essentially constant between 150 and 300 K. We believe it to be significant that the negative high-temperature slope of W_{ei} is consistent with the $-BT^2$ term used in fitting the resistivity in Sec. IV A. If we assume that $\Delta\rho$ is connected to ΔW through the Lorenz number L_0 we have

$$\Delta\rho = L_0 T \Delta W \approx -2 \times 10^{-13} T^2. \quad (14)$$

The value of $\Delta\rho$ calculated in this manner is about 15%

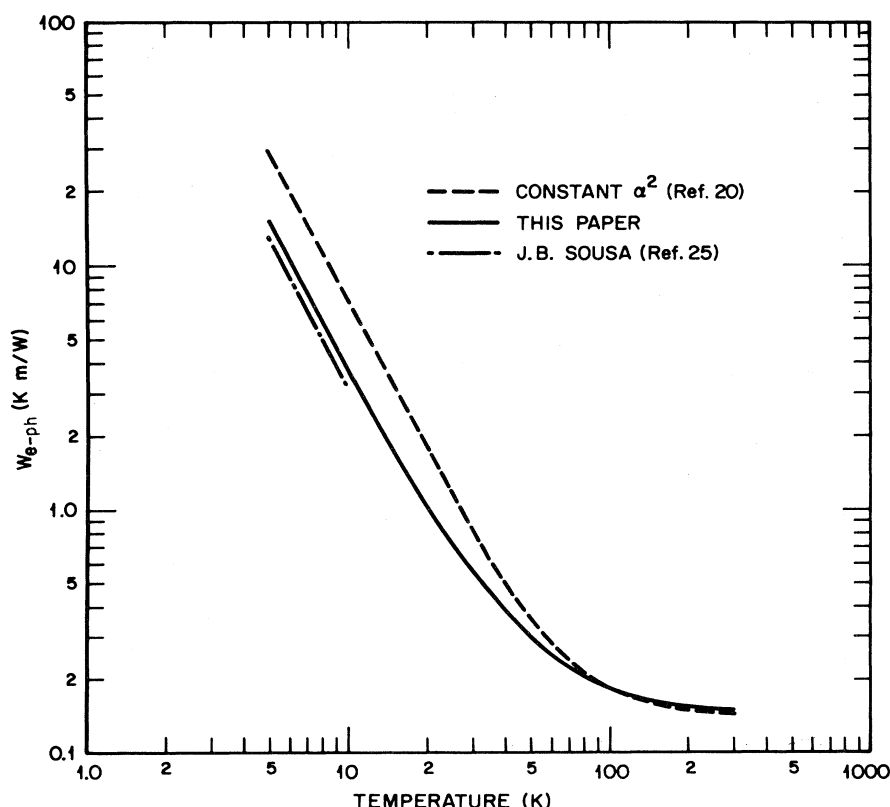


FIG. 3. Temperature variation of the resistance to phonon energy transport in niobium caused by electron-phonon scattering. The solid line was obtained from Eq. (11) as described in the text.

larger than the values of BT^2 shown in Table III. We interpret this result as an indication that the “negative deviation from linearity” or “saturation” effect is observable at temperatures as low as 100 K in Nb.

The possible persistence of the DFL mechanism to relatively low temperatures complicates the comparison be-

tween the first-principles calculation⁴ and the experimental W_{ei} values, because the theory does not contain any elements which could generate a DFL. Adjusting the experimental W_{ei} values upward to remove the hypothesized linear, negative DFL contribution to W_{ei} produces a curve which is in remarkably ($\pm 1\%$) good agreement with the first-principles calculation over the whole temperature range. This suggests that the rigid muffin-tin approximation may not overestimate the electron-phonon interaction at high temperatures as was originally suggested by Butler.¹⁸ According to this interpretation the rigid muffin-tin calculations only appear to overestimate the basic electron-phonon interaction because the electrical and thermal resistivities are depressed by a DFL of unknown origin.

We can only speculate about the origin of the DFL. Part of it, no doubt, arises from “phonon softening”—a misnomer in this case since the phonon frequencies of Nb actually increase with increasing temperatures. This increase in the phonon frequencies causes the electron-phonon interaction to decrease and thereby decreases the electrical and thermal resistivities. Allen³¹ has estimated that this “phonon hardening” may explain about one-third of the effect at 1000 K in Nb. He also investigated “Mott-Fermi smearing,” the fact that the conductivity at elevated temperatures depends not just on the Fermi energy electronic structure, but on the electronic structure within an energy range of approximately $3k_B T$ about ϵ_F .

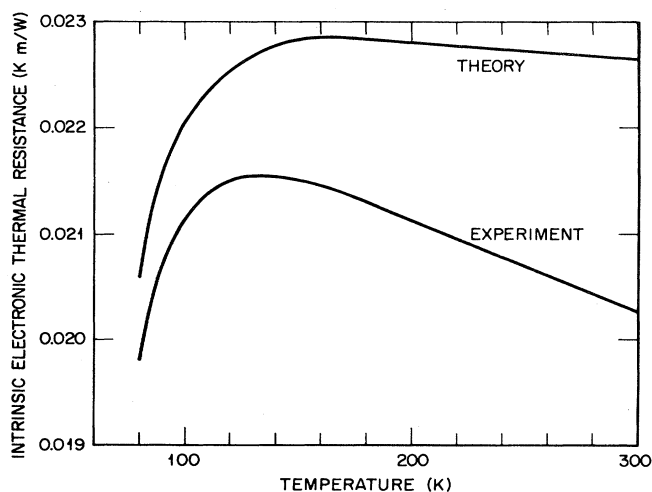


FIG. 4. Comparison of experimental and theoretical values for the intrinsic electronic thermal resistance (λ_e^{-1}) of niobium.

Allen calculated that this effect was small and of the wrong sign to explain the DFL in Nb, although this conclusion was later challenged by Laubitz *et al.*¹³ Allen³² and Chakraborty³³ have suggested that the DFL's of Nb and many other transition metals and compounds result at least in part from interband transitions. These purely quantum-mechanical transitions provide an additional channel for electrical conduction not included in semiclassical Boltzmann theory. Equation (14) which we observe to be approximately valid would be consistent with the phonon-hardening and interband transition explanation for the DFL.

The experimental [from Eqs. (4) and (5)] and theoretical (from Ref. 4) intrinsic electronic Lorenz functions are compared in Fig. 5. The experimental curve lies about 3–4% above the prediction. When used in conjunction with the λ and ρ of the Nb sample, the theoretical L curve also yields an estimate of λ_{ph} of Nb. This would be justified if the theory yields errors in λ_e and $T\rho^{-1}$ which compensate. This estimate of λ_{ph} , which is somewhat more subject to the experimental λ and ρ uncertainties, is discussed in the final section of this paper.

F. Comparison of λ_{ph} results

The theoretical W_{e-ph} prediction shown in Fig. 3 is about 35% less than the experimental value shown in Fig. 2 and Eq. (9). This is similar to the result obtained for Ta,² and enhances our belief that there is some physical basis for the difference. Figure 2 shows that the scatter of the four sets of calculated λ_{ph}^{-1} values is only about $\pm 10\%$, but an error analysis² indicates an uncertainty of about $\pm 40\%$. This is just sufficiently large to include the theoretical value.

Attempts to reconcile the experimental and theoretical values of W_{e-ph} by refining the analysis were only partially successful. The assumed additivity [Eq. (6)] of the thermal resistivities is incorrect in principle, as emphasized by Callaway,³⁴ due to the different frequency dependencies of the phonon-electron, phonon-phonon, and

phonon-impurity scattering rates. However, a more proper calculation in which the frequency-dependent scattering rates were added and the sum inverted to obtain the net phonon lifetime as a function of frequency did not yield appreciably different results for B . The point-defect scattering rate is rather uncertain, so we tried increasing it by a factor of 5. The result is shown in Fig. 6. It is close to the original result at low temperatures, does not exhibit a maximum, and considerably ($\times 2$) exceeds the theoretical λ_{ph} prediction at room temperature. Thus although evaluation of the local strain scattering of phonons continues to be an important unsolved problem, Fig. 6 shows that it cannot be used to successfully shift the experimental results. Finally, an examination of dislocation scattering results and theories³⁵ leads us to believe that this scattering would be less than 1% in our well-annealed, large grain size, cast samples.

The possible discrepancy between theory and experiment requires a closer scrutiny of the theoretical calculation. Errors in the theoretical results arising from the assumed phonon dispersion [Eq. (13)] are probably small. One possible source of error in the calculation is our use of rigid muffin-tin matrix elements. Insight into the adequacy of this approximation can be gained by comparing the results of rigid muffin-tin calculations for the electrical resistivity and for the superconducting spectral function, $\alpha^2(\omega)F(\omega)$, with the corresponding experimental results. The results of such comparisons indicate that although the rigid muffin-tin matrix elements are possibly too weak at low frequency their average over all frequencies are approximately correct.

The phonon-phonon scattering correction, which was obtained from Eq. (8), may be responsible for part of the discrepancy. There are three concerns: (1) estimates of the inherent strength of the U -process scattering via Eq. (8), (2) failure of the additive resistance approximation [Eq. (9)], and (3) the role of N processes. Including the theoretical electron-phonon scattering in Callaway's³⁴ for-

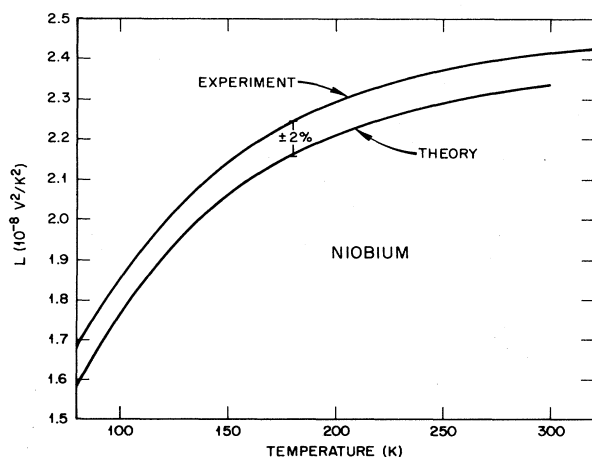


FIG. 5. Comparison of experimental and theoretical values of the electronic Lorenz function, L , of niobium.

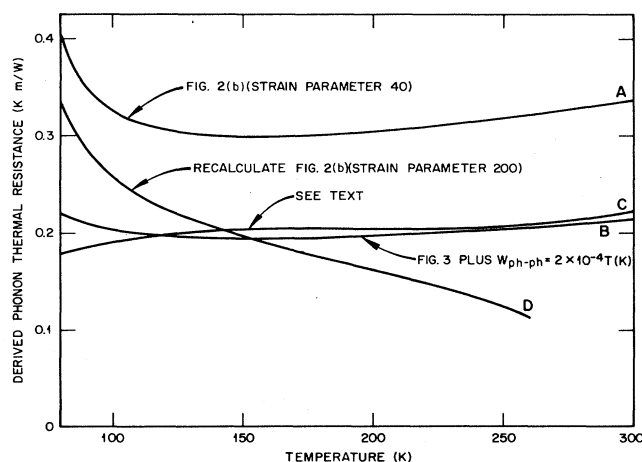


FIG. 6. Temperature variation of values of λ_{ph}^{-1} for niobium. Curve A shows our best experimental estimate and curve B is the result obtained from a first-principles theoretical calculation.

mula shows that the additive resistance approximation underestimates the resistance by about 10%, and a further increase can be calculated by assuming that scattering by N processes is much stronger than the U -process term. As mentioned previously, the magnitude of the U -process scattering is also uncertain by a factor of about 2. Retaining the prediction of Eq. (8) and assuming strong N processes with Callaway's equation yields a phonon conductivity which is about 80% of the experimental result.

Figure 6 shows that the λ_{ph} curve obtained by combining the theoretical L calculations (Fig. 5) with the λ and ρ data for Nb (curve C) is in remarkably good agreement with the result calculated from Eq. (11). This supports the theory, and the only misgivings are that the temperature dependence is not quite correct and the λ_{ph} values are more subject to experimental errors.

To summarize, at present we do not know how to improve the experimental λ_{ph} value. The rather large error bounds do, however, include the theoretical result. The prospects for calculating λ_{ph} look promising. The λ_{ph}

values calculated here are in good agreement with values derived from a mixed experimental and theoretical technique in which the calculated electronic Lorenz number is used with the experimental electrical resistivity to determine the electronic thermal conductivity which is subtracted from the total conductivity to determine λ_{ph} .

Further work on other systems should be done to confirm our ability to calculate λ_{ph} from first principles. Molybdenum and vanadium appear to be good candidates for such a study because for them λ_{ph} should be a larger fraction of the total thermal conductivity allowing a more accurate experimental determination of λ_{ph} .

ACKNOWLEDGMENTS

The experimental assistance of F. J. Weaver and D. W. Yarbrough is greatly appreciated. This research was sponsored by the Division of Materials Sciences, U.S. Department of Energy, under Contract No. W-7405-eng-26 with the Union Carbide Corporation.

- ¹R. K. Williams, D. W. Yarbrough, J. S. Masey, T. K. Holder, and R. S. Graves, *J. Appl. Phys.* **52**, 5167 (1981).
- ²R. K. Williams, R. S. Graves, T. L. Hebble, D. L. McElroy, and J. P. Moore, *Phys. Rev. B* **26**, 2932 (1982).
- ³J. P. Moore, R. S. Graves, and R. K. Williams, *High Temp. High Pressures* **12**, 579 (1980).
- ⁴F. J. Pinski, P. B. Allen, and W. H. Butler, *Phys. Rev. B* **23**, 5080 (1981).
- ⁵R. E. Reed, in *Proceedings of the 2nd International Conference on Electron and Ion Beam Science and Technology*, edited by R. Bakish (IMD-AIME, New York, 1969), p. 225.
- ⁶G. K. White and S. B. Woods, *Philos. Trans. R. Soc. London Ser. A* **251**, 273 (1959).
- ⁷B. A. Merisov, V. I. Khotkevich, G. M. Zlobintsev, and V. V. Kozine, *Inzh.—Fiz. Zh.* **12**, 675 (1967).
- ⁸C. Y. Ho, R. W. Powell, and P. E. Liley, *J. Phys. Chem. Ref. Data* **3**, Suppl. 1, 470 (1974).
- ⁹R. K. Williams, R. S. Graves, and J. P. Moore, ORNL Report No. 5313 (unpublished).
- ¹⁰J. P. Moore, D. L. McElroy, and R. S. Graves, *Can. J. Phys.* **45**, 3849 (1967).
- ¹¹J. P. Moore, R. K. Williams, and R. S. Graves, *Rev. Sci. Instrum.* **45**, 87 (1974).
- ¹²P. B. Allen, *Phys. Rev. Lett.* **37**, 1638 (1976).
- ¹³M. J. Laubitz, C. R. Leavens, and R. Taylor, *Phys. Rev. Lett.* **39**, 225 (1977).
- ¹⁴B. M. Powell, P. Martel, and A. D. B. Woods, *Can. J. Phys.* **55**, 1601 (1977).
- ¹⁵M. Ishikawa and R. L. Cappelletti, *J. Low Temp. Phys.* **20**, 407 (1975).
- ¹⁶G. Grimvall, *Phys. Scr.* **14**, 63 (1976).
- ¹⁷W. H. Butler, *Phys. Rev. B* **15**, 5267 (1977).
- ¹⁸W. H. Butler, in *Superconductivity in d- and f-Band Metals*, edited by H. Suhl and M. B. Maple (Academic, New York, 1980), p. 443.
- ¹⁹F. J. Blatt, P. J. Schroeder, C. L. Foiles, and D. Greig, *Thermoelectric Power of Metals* (Plenum, New York, 1976), p. 28.
- ²⁰J. M. Ziman, *Electrons and Phonons* (Oxford at the Clarendon Press, London, 1960), p. 385.
- ²¹R. E. B. Makinson, *Proc. Cambridge Philos. Soc.* **34**, 474 (1938).
- ²²W. H. Butler and R. K. Williams, *Phys. Rev. B* **18**, 6483 (1978).
- ²³M. Roufosse and P. G. Klemens, *Phys. Rev. B* **7**, 5379 (1973).
- ²⁴C. L. Julian, *Phys. Rev.* **137**, A128 (1965).
- ²⁵B. Abeles, *Phys. Rev.* **131**, 1906 (1963).
- ²⁶J. P. Moore, R. K. Williams, and R. S. Graves, *Phys. Rev. B* **11**, 3107 (1975).
- ²⁷J. B. Sousa, *J. Phys. C* **2**, 629 (1969).
- ²⁸W. H. Butler, F. J. Pinski, and P. B. Allen, *Phys. Rev. B* **19**, 3708 (1979).
- ²⁹F. J. Pinski and W. H. Butler, *Phys. Rev. B* **19**, 6010 (1979).
- ³⁰W. H. Butler, H. G. Smith, and N. Wakabayashi, *Phys. Rev. Lett.* **39**, 1004 (1977).
- ³¹P. B. Allen, *Phys. Rev. Lett.* **37**, 1638 (1976).
- ³²P. B. Allen, in *Superconductivity in d- and f-Band Metals*, edited by H. Suhl and M. B. Maple (Academic, New York, 1980), pp. 291–304.
- ³³B. Chakraborty and P. B. Allen, *Phys. Rev. Lett.* **42**, 736 (1979).
- ³⁴J. Callaway, *Phys. Rev.* **122**, 787 (1961).
- ³⁵P. G. Klemens, *Solid State Physics*, edited by F. Seitz and D. Turnbull (Academic, New York, 1958), Vol. 7, p. 1.
- ³⁶P. G. Klemens, *Solid State Phys.* **7**, 1 (1958).